Letters

Ultralow-Loss Substrate-Integrated Waveguides in Glass-Based Substrates for Millimeter-Wave Applications

Atom O. Watanabe, *Student Member, IEEE*, Bijan K. Tehrani, Tomonori Ogawa, Pulugurtha Markondeya Raj, Manos M. Tentzeris, *Fellow, IEEE*, and Rao R. Tummala, *Life Fellow, IEEE*

***Abstract*— This letter, for the first time, presents low-loss substrate-integrated waveguides (SIWs) in fused silica and borosilicate glass and a comparison of their performance with various organic-based low-loss substrates for millimeter-wave applications. Utilizing ring resonators designed for frequencies in the 5G New Radio (NR) n257 band (26.5–29.5 GHz), this letter begins with the determination of the dielectric constant of fused silica to model SIWs. This letter also introduces the designs of SIWs that are fed by conductor-backed coplanar waveguides and discusses the fabrication and measurement results with deembedding analysis. In addition to the excellent correlation between simulations and measurements, the characterization results show more than 2× reduction in the insertion loss compared to those of low-loss organic-based SIWs at the 28-GHz frequency band.**

***Index Terms*— 5G, fused silica, glass, low loss, millimeter wave (mm-wave), packaging.**

I. Introduction

THE evolution of 5G communications has been leading to new challenges in millimeter (mm)-wave packaging technologies [1]. To address the challenges such as signal loss, electromagnetic interference, size reduction with direct antenna-integrated packages, and thickness minimization, substrate-integrated waveguide (SIW) strategy is gaining attention for low-profile waveguides that are fabricated into a dielectric substrate. This approach uses package-integrated antennas [2], bandpass filters [3], power dividers [4], and other passive elements. As the SIW is a rectangular waveguide formed by a dielectric, two metal planes, and metallized by arrays, the electromagnetic wave propagates through the dielectric medium formed by the substrate. To achieve a high Q factor or low-loss signal transmission, the dielectric dissipation factor ($\tan\delta$) is extremely critical to minimize the signal attenuation in the SIW.

Conventional methods utilize organic substrates such as liquid-crystal polymers (LCPs) [5], ceramic hydrocarbons [6], and polytetrafluoroethylenes (PTFEs) [7], [8] because of their large-area low-cost manufacturing infrastructure cost and low dissipation factor. These substrates, however, lead to several fundamental barriers and challenges to achieve high precision and tolerance that are required for millimeter-wave (mm-wave) components in the dimension of a few microns. As an ideal evolution to address these challenges, glass-based substrates are emerging because of their ability to form fine-pitch lines and spaces and through vias, robustness against high temperature and humidity, dimensional stability, matched coefficient of thermal expansion (CTE) with silicon dies, and large-area low-cost panel-scale processability [9], [10]. However, borosilicate glass with low CTE is prone to losses because of added ionic contents that cause dipole relaxation in mm-wave frequencies. A low-loss fused-silica glass is developed to address these limitations, while retaining all the advantages of borosilicate glass.

This letter discusses ultralow-loss SIWs fed by coplanar waveguides in thin borosilicate glass and fused silica substrates in the 5G New Radio (NR) n257 band (26.5–29.5 GHz) for 5G/mm-wave applications. Section II discusses the characterization of the dielectric properties (i.e., relative permittivity ε_r and dissipation factor $\tan\delta$). Section III focuses on the designs of the SIW based on cutoff frequencies, calibration methodology, and the dimensions of elements. Finally, the insertion losses in borosilicate glass and fused silica are discussed.

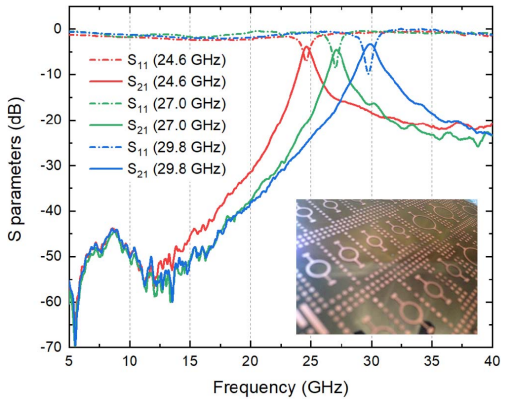

Fig. 1. Measured frequency responses of the ring resonators designed at three frequencies with an inset figure of the fabricated test vehicle.

II. Ring-Resonator Characterization of Fused Silica

To accurately characterize the dielectric properties of fused silica, which is widely used for high-performance optical fibers, ring resonators that characterize relative permittivity ε_r and dissipation factor $\tan\delta$ were designed at 24.6, 27.0, and 29.8 GHz. The ring resonators were fabricated directly on fused silica, as depicted in the inset of Fig. 1 using the semiadditive patterning (SAP) process. The measured return loss and insertion loss of the ring resonators designed for the three frequencies are shown in Fig. 1. From the resonant frequencies and the 3-dB bandwidths, relative permittivity and dissipation factor were derived [11], [12]. The dielectric properties are calculated from the dielectric loss and conductor loss based on surface roughness and

Manuscript received September 22, 2019; revised December 24, 2019; accepted January 14, 2020. Date of publication January 21, 2020; date of current version March 10, 2020. Recommended for publication by Associate Editor L.-T. Hwang upon evaluation of reviewers' comments. *(Corresponding author: Atom O. Watanabe.)*

Atom O. Watanabe, Bijan K. Tehrani, Manos M. Tentzeris, and Rao R. Tummala are with the School of Electrical and Computer Engineering, Georgia Institute of Technology, Atlanta, GA 30332 USA (e-mail: atom@gatech.edu).

Tomonori Ogawa is with Asahi Glass Company (AGC), Tokyo 100-0005, Japan.

Pulugurtha Markondeya Raj is with the School of Electrical and Computer Engineering, Georgia Institute of Technology, Atlanta, GA 30332 USA, and also with the Department of Biomedical Engineering, Florida International University, Miami, FL 33174 USA.

Color versions of one or more of the figures in this letter are available online at http://ieeexplore.ieee.org.

Digital Object Identifier 10.1109/TCPMT.2020.2968305

TABLE I
MEASURED DIELECTRIC PROPERTIES OF FUSED SILICA

	25 GHz	27 GH	30 GHz
Dielectric constant, ε_r	3.85	3.78	3.74
Dissipation factor, tan$\delta(\times 10^{-4})$	3.29	3.26	3.83

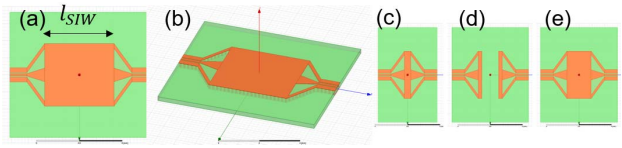

Fig. 2. SIW designs in HFSS with (a) top view with a length, l_{SIW}, of 4 mm and widths of 3.08 and 3.68 mm for borosilicate glass and fused-silica glass, respectively. (b) 3-D view and high-accuracy precision method with (c) through, (d) reflect, and (e) line.

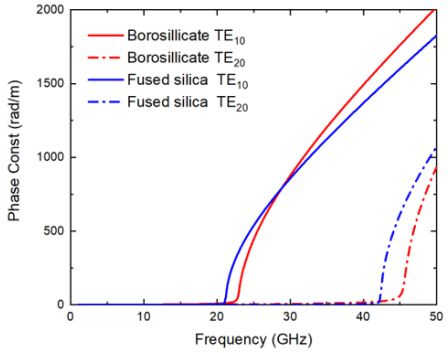

Fig. 3. Cutoff frequency of the TE_{10} and TE_{20} modes for borosilicate glass and fused silica.

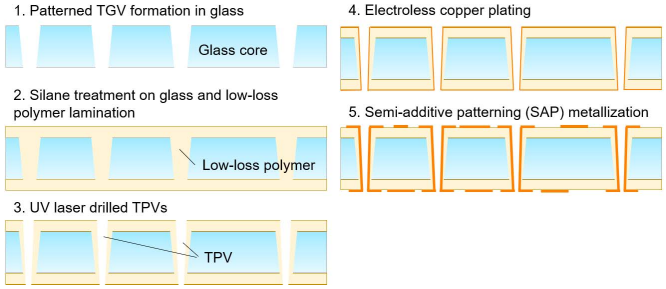

Fig. 4. Process flow for semiadditive copper patterning [14] on a glass core laminated with thin low-loss dielectric polymer films.

metal conductivity. The derived results are listed in Table I, showing approximately ten times lower dissipation factors than other low-loss organic dielectric materials used for 5G/mm-wave applications. This result from the ring-resonator characterization using a thin substrate is consistent with the reported dielectric properties of bulk fused silica [13].

III. MODELING AND DESIGN OF SIWS

Based on the characterized dielectric properties, we designed conductor-backed coplanar waveguide (CPWG)-fed SIWs for borosilicate glass and fused-silica substrates laminated with 15-μm low-loss dielectric films, as shown in Fig. 2(a) and (b). To deembed the insertion loss of the CPWG, T(through)–R(reflect)–L(line) structures were also designed, as shown in Fig. 2(c)–(e). The detailed simulations were performed using an electromagnetic finite-element method solver, HFSS. The SIW consists of two metal planes and two arrays on through-glass vias (TGVs) to form a rectangular parallelepiped. In the waveguide, only the TE_{10} (TE: transverse electric) mode propagates in the waveguide, whereas the TE_{20} mode is cutoff in the

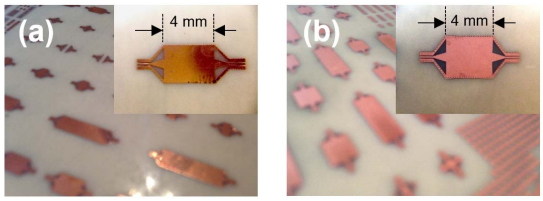

Fig. 5. Fabricated SIWs with TRL calibration structures in (a) borosilicate glass and (b) fused silica substrates.

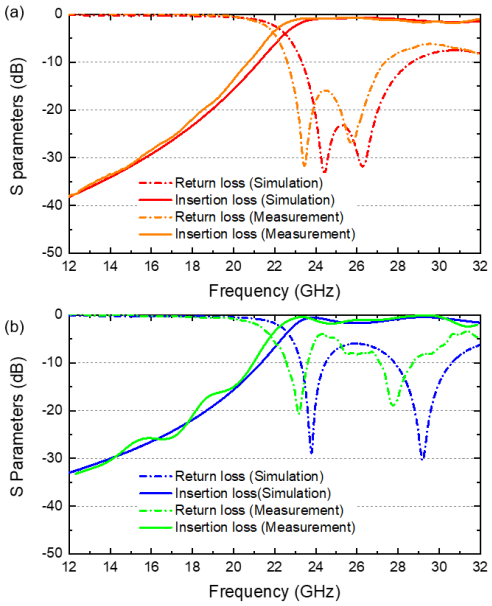

Fig. 6. Simulated and measured results of the fabricated SIWs with CPWG and the transition between them.

TABLE II
COMPARISON OF DEEMBEDDED INSERTION LOSSES BETWEEN SIMULATIONS AND MEASUREMENTS

	Borosilicate glass		Fused silica	
	dB	dB/mm	dB	dB/mm
Simulation	-0.552	-0.138	-0.092	-0.023
Measurement	-0.484	-0.121	-0.071	-0.018

target frequency range, 24–42 GHz, as shown in Fig. 3. Equation (1) indicates that the selection of TE_{n0} modes allows us to design ultrathin waveguides in packaging substrates. The length of SIWs l_{SIW} is 4 mm throughout this letter, whereas the thicknesses of borosilicate glass and fused silica are 100 and 210 μm, respectively,

$$f_{c,mn} = \frac{1}{2\pi\sqrt{\mu\epsilon}}\sqrt{\left(\frac{m\pi}{w}\right)^2 + \left(\frac{n\pi}{h}\right)^2}. \quad (1)$$

IV. FABRICATION AND CHARACTERIZATION

A. Fabrication of SIWs in Borosilicate Glass and Fused Silica

To verify the designed models discussed in III, SIWs are fabricated through a SAP process as illustrated in Fig. 4. The lamination of a thin low-loss polymer with a relative dielectric constant of 3.3 and a dissipation factor of 0.0044 on glass substrates enhances the adhesion strength of copper to the substrate and mitigates the residual stress between the core substrate and copper patterns, thus preventing copper traces from delaminating from the substrate. This patterning process enables high tolerance below 2 μm on glass-based substrates, which minimizes the impedance deviation from designs and thus achieve high model-to-hardware correlation. The fabricated SIWs are shown in Fig. 5.

TABLE III
COMPARISON OF THE INSERTION LOSS OF SIWs WITH VARIOUS PACKAGING SUBSTRATES

	[5]	[6]	[7]	[8]	This work	This work
Material	LCP	Hydrocarbon ceramic	PTFE	PTFE	Borosilicate glass	Fused silica
Dielectric constant, ε_r	3.16	3.38	2.2	2.94	5.4	3.78
Dissipation factor, tanδ	0.0049	0.0027	0.0009	0.0012	0.006	0.0003
CTE (ppm/K)	17	40	125	12	3.8	0.6
Thickness (μm)	127	1524	254	508	100	210
Frequency (GHz)	50–70	7–14	50–75	50–75	24–40	24–40
Insertion loss (dB/mm)	0.12	0.038	0.042	0.035	0.158	0.018

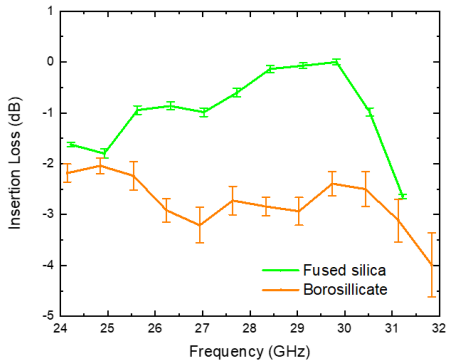

Fig. 7. Measured results focusing on the 28-GHz frequency band.

B. Characterization Results and Analysis

This section discusses the characterization results of the fabricated SIWs. The measurements are performed through a vector network analyzer and a pair of GSG probes that are accurately calibrated up to 40 GHz. Fig. 6 shows the intended cutoff frequency at around 24 GHz and excellent correlation between simulations and measurements of the CPWG-fed SIWs for both borosilicate glass and fused silica. To obtain precise insertion losses at the target frequency, 28 GHz, the vector network analyzer was recalibrated in a narrow frequency range. The measured frequency responses are plotted in Fig. 7 along with their averages and standard deviations computed from eight samples in each substrate.

Based on the SIW results and measured TRL structures, the insertion losses of SIWs were deembedded from CPWG and the transition between CPWG and SIWs. The deembedded results are listed in Table II, showing an insertion loss below 0.02 dB/mm with the fused silica substrate.

Table III lists the comparison of insertion losses of SIWs with various low-loss substrates. While the thickness reduction of substrates causes an increase in insertion losses, the comparison indicates that borosilicate glass has the potential to reduce thickness. The fused silica substrates achieve 0.018 dB/mm, which is 2× less in insertion loss compared to that of the organic-based SIWs. This low-loss SIW in fused silica is predominantly enabled by its low dissipation factor. In addition, the stack-up of a fused silica core laminated with 15-μm low-loss dielectric films offer higher adhesion, lower interfacial stress, and higher reliability than metallization directly on a fused silica glass core [13].

V. CONCLUSION

Innovative low-loss glass substrates are developed from fused silica as a replacement to traditional glass substrates for packaging. This letter begins with the characterization of the dielectric constants of these novel silica substrates. The characterization results show ultralow dissipation factors around 28 GHz. The second part demonstrates SIWs for the 28-GHz band with borosilicate glass and fused silica and compares them with other leading-edge low-loss organic-based substrates. The deembedded insertion loss based on TRL calibrations shows 0.018 dB/mm. SIWs using borosilicate glass or fused silica can be extended to other applications such as low-pass or bandpass filters and low-footprint package-integrated antennas. The research highlights the potential of the glass-based substrates as a thin core substrate for mm-wave applications.

REFERENCES

[1] V. Gjokaj, J. Doroshewitz, J. Nanzer, and P. Chahal, "A design study of 5G antennas optimized using genetic algorithms," in *Proc. IEEE 67th Electron. Compon. Technol. Conf. (ECTC)*, Orlando, FL, USA, May/Jun. 2017, pp. 2086–2091.

[2] S. Park and S. Park, "LHCP and RHCP substrate integrated waveguide antenna arrays for millimeter-wave applications," *IEEE Antennas Wireless Propag. Lett.*, vol. 16, pp. 601–604, 2017.

[3] R. Bowrothu, S. Hwangbo, T. Schumann, and Y. Yoon, "28 GHz through glass via (TGV) based band pass filter using through fused silica via (TFV) technology," in *Proc. IEEE 69th Electron. Compon. Technol. Conf. (ECTC)*, Las Vegas, NV, USA, May 2019, pp. 695–699.

[4] K. Song, F. Xia, Y. Zhou, S. Guo, and Y. Fan, "Microstrip/slotline-coupling substrate integrated waveguide power divider with high output isolation," *IEEE Microw. Wireless Compon. Lett.*, vol. 29, no. 2, pp. 95–97, Feb. 2019.

[5] K. Yang, S. Pinel, K. Kim, and J. Laskar, "Millimeter-wave low-loss integrated waveguide on liquid crystal polymer substrate," in *IEEE MTT-S Int. Microw. Symp. Dig.*, San Francisco, CA, USA, Jun. 2006, pp. 965–968.

[6] R. Kazemi, A. E. Fathy, S. Yang, and R. A. Sadeghzadeh, "Development of an ultra wide band GCPW to SIW transition," in *Proc. IEEE Radio Wireless Symp.*, Santa Clara, CA, USA, Jan. 2012, pp. 171–174.

[7] X. Peng, J. Chen, H. Tang, D. Hou, P. Yan, and W. Hong, "Broadband and low-loss rectangular waveguide to substrate integrated waveguide transition with fin line," in *IEEE MTT-S Int. Microw. Symp. Dig.*, Phoenix, AZ, USA, May 2015, pp. 1–3.

[8] I. Mohamed and A. R. Sebak, "Broadband transition of substrate-integrated waveguide-to-air-filled rectangular waveguide," *IEEE Microw. Wireless Compon. Lett.*, vol. 28, no. 11, pp. 966–968, Nov. 2018.

[9] W. T. Khan, J. Tong, S. Sitaraman, V. Sundaram, R. Tummala, and J. Papapolymerou, "Characterization of electrical properties of glass and transmission lines on thin glass up to 50 GHz," in *Proc. IEEE 65th Electron. Compon. Technol. Conf. (ECTC)*, San Diego, CA, USA, May 2015, pp. 2138–2143.

[10] A. Watanabe *et al.*, "Leading-edge and ultra-thin 3D glass-polymer 5G modules with seamless antenna-to-transceiver signal transmissions," in *Proc. IEEE 68th Electron. Compon. Technol. Conf. (ECTC)*, San Diego, CA, USA, May 2018, pp. 2026–2031.

[11] P. Bernard and J. Gautray, "Measurement of dielectric constant using a microstrip ring resonator," *IEEE Trans. Microw. Theory Techn.*, vol. 39, no. 3, pp. 592–595, Mar. 1991.

[12] J.-. Heinola, P. Silventoinen, K. Latti, M. Kettunen, and J.-P. Strom, "Determination of dielectric constant and dissipation factor of a printed circuit board material using a microstrip ring resonator structure," in *Proc. 15th Int. Conf. Microw., Radar Wireless Commun.*, Warsaw, Poland, vol. 1, 2004, pp. 202–205.

[13] Y. Uemichi, O. Nukaga, X. Han, R. Hosono, N. Guan, and S. Amakawa, "Characterization of 60-GHz silica-based post-wall waveguide and low-loss substrate dielectric," in *Proc. Asia–Pacific Microw. Conf. (APMC)*, New Delhi, India, 2016, pp. 1–4.

[14] P. M. Raj *et al.*, "'Zero-undercut' semi-additive copper patterning—a breakthrough for ultrafine-line RDL lithographic structures and precision RF thinfilm passives," in *Proc. IEEE 65th Electron. Compon. Technol. Conf. (ECTC)*, San Diego, CA, USA, May 2015, pp. 402–405.